A NEW INTERPRETATION OF THE X-RAY SPECTRAL VARIABILITY OF NGC 4051

G. Ponti[1,2,3], G. Miniutti[1], M. Cappi[3], L. Maraschi[4], A.C. Fabian[1], and K. Iwasawa[1]

[1]Institute of Astronomy, Madingley Road, Cambridge CB3 0HA
[2]Dipartimento di Astronomia, Università di Bologna, Via Ranzani 1, I–40127, Bologna, Italy
[3]INAF–IASF Sezione di Bologna, Via Gobetti 101, I–40129, Bologna, Italy
[4]Osservatorio Astronomico di Brera, via Brera 28, 20121 Milan, Italy

ABSTRACT

We study the X–ray spectral variability of the Narrow Line Seyfert 1 galaxy NGC 4051 as observed during two *XMM–Newton* observations. The data show evidence for a neutral and constant reflection component and for constant emission from photoionized gas. The nuclear emission can be modelled both in terms of a "standard model" (pivoting power law plus a black body component for the soft excess) and of a two–component one (power law plus ionized reflection from the accretion disc). Both models reproduce the source spectral variability and cannot be distinguished on a statistical ground. The distinction has thus to be made on a physical basis. The standard model results indicate that the soft excess does not follow the standard black body law. The resulting temperature is consistent with being constant and has the same value as observed in PG quasars which have a much larger black hole mass than NGC 4051. Moreover, although the spectral slope is correlated with flux (consistent with spectral pivoting) the hardest photon indexes are so flat as to require rather unusual scenarios. Furthermore, the very low flux states exhibit an inverted Γ–flux behaviour which disagrees with a simple pivoting interpretation. These problems can be solved in terms of the two–component model in which the soft excess is not thermal, but due to the ionized reflection component. The variability of the reflection component from the inner disc closely follows the predictions of the light bending model, suggesting that most of the primary nuclear emission is produced in the very innermost regions, only a few gravitational radii from the central black hole.

Key words: X-rays; galaxies: active; galaxies: individual: NGC 4051.

1. INTRODUCTION

NGC 4051 is a nearby (z=0.0023) low–luminosity Narrow–Line Seyfert 1 (NLS1) galaxy which exhibits extreme X–ray variability in flux and spectral shape on both long and short timescales. The source sometimes enters relatively long and unusual low flux states in which the hard spectrum becomes very flat ($\Gamma \sim 1$) while the soft band is dominated by a much steeper component ($\Gamma \sim 3$, or blackbody with $kT \sim 0.12$ keV). Most remarkable is the 1998 *BeppoSAX* observation reported by Guainazzi et al (1998) in which the source reached its minimum historical flux state and the overall spectrum was best explained by assuming that the nuclear emission had switched off leaving only a reflection component from distant material.

NGC 4051, like many other Seyfert 1 and NLS1 galaxies, shows a 2–10 keV spectral slope that is well correlated with flux. However, the correlation is not linear with the slope hardening rapidly at low fluxes and reaching an asymptotic value at high fluxes (see e.g. Lamer et al 2003). This behaviour might be due to flux–correlated variations of the power law slope produced in a corona above an accretion disc as originally proposed by Haardt & Maraschi (1991; 1993) and related to changes in the input soft seed photons (e.g. Haardt, Maraschi & Ghisellini 1997, Poutanen & Fabian 1999). On the other hand, such slope–flux behaviour can be explained in terms of a two–component model (Shih, Iwasawa & Fabian 2002) in which a constant slope power law varies in normalisation only, while a harder component remains approximately constant hardening the spectral slope at low flux levels only, when it becomes prominent in the hard band.

Uttley et al (2004) have analysed the same *XMM–Newton* data we are presenting here. They showed that the source spectral variability is consistent with a Comptonization scenario and that the same process causing the spectral variability in high and intermediate flux states continues to operate even at the very low flux levels probed by the *XMM–Newton* data). This evidence seems to challenge the interpretation of the spectral variability as due to variable absorption by a substantial column of gas partially covering the source and affecting the spectral shape above 3 keV (Pounds et al. 2004).

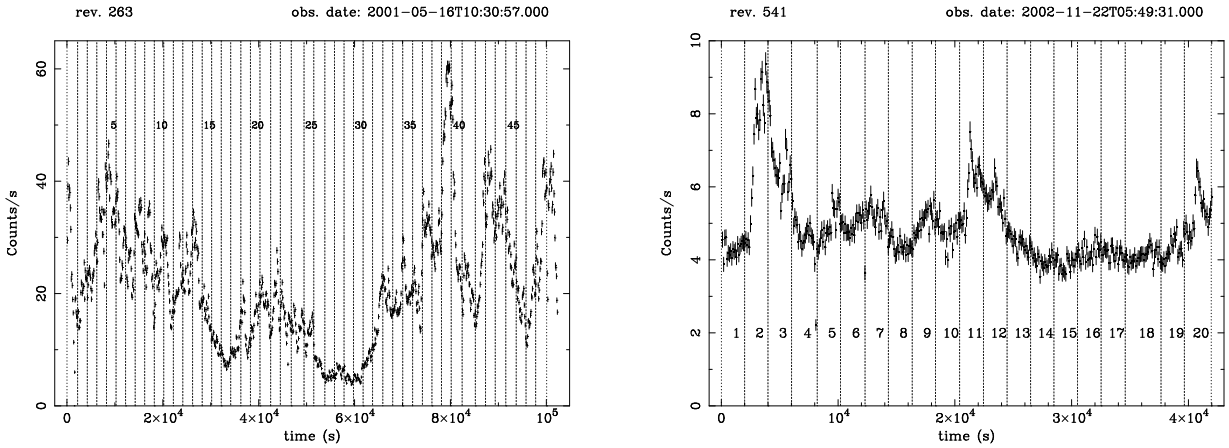

Figure 1. The broadband 0.2–10 keV XMM–Newton EPIC–pn light curves of NGC 4051 for the first (left panel, rev. 263) and the second (right panel, rev. 541) observations. The 2 ks time slices used in the time–resolved spectroscopic analysis are also shown.

2. SPECTRAL VARIABILITY: RMS SPECTRA

NGC 4051 has been observed twice by *XMM-Newton*. During the first observation (rev. 263, 2001 May) the source flux was comparable to the historical average, while during the second (rev. 541, 2002 November) it was much lower. The *XMM–Newton* broadband light curve of NGC 4051 (see Fig. 1) exhibits an extraordinary variability with variations up to a factor of 3 in few thousands seconds. We observe that not only the flux, but also the spectral slope changes in the same short timescale. To study the spectral variability, we start our analysis calculating the RMS spectrum, which measures the total amount of variability as a function of energy (Edelson et al. 2002; Vaughan et al. 2004; Ponti et al. 2004).

During the high flux observation of rev. 263 (Fig. 2) the variability rapidly increases toward softer energies, i.e. the broadband emission tends to steepen as it brightens. Some reduction in the variability is seen below about 800 eV followed by a plateau below 500 eV. A similar RMS shape has been observed in other sources (Ponti et al. 2005; Vaughan et al. 2003; Vaughan et al. 2004) and the two simplest explanations for the broadband trend invoke either spectral pivoting of the variable component, or the two–component model (see e.g Markowitz, Edelson & Vaughan 2003). Another important feature of the RMS spectrum is a drop of variability at 6.4 keV. Such a drop shows that the narrow Fe line (and therefore the associated reflection continuum) is much less variable than the continuum indicating an origin in distant material. Some structure is also present around 0.9 keV, with the possible presence of either a drop at that energy or two peaks.

The right panel of Figure 1 shows the RMS spectrum obtained for the low flux observation (rev 541). The variability below 3 keV is strongly suppressed with respect to the high flux observation. Moreover, the shape of the RMS spectrum is totally different and rather unusual. The trend of increasing variability toward softer energies breaks down completely and the most striking feature is the marked drop of variability around 0.9 keV. This feature, as well as the other drop of variability at $\sim$0.55 keV, could have the same nature as the structure seen in the high flux RMS spectrum, but is much more significant and prominent here. As in the high flux observation, the variability is also suppressed around 6.4 keV.

The drops of variability at the energy of the narrow component of the Fe K line suggest that it comes from material distant from the variable illuminating source. In the time–averaged spectra the narrow component of the Fe line is clearly detected. In the low flux one, the line is unresolved, has an energy of 6.42 ± 0.015 keV, a flux of $(1.5 \pm 0.2) \times 10^{-5}$ ph s^{-1} cm^{-2}, and an equivalent width of about 260 eV. The line energy and flux are consistent with measurements obtained in the high flux observation and also with previous data from *Chandra* (Collinge et al 2001) and *BeppoSAX* (Guainazzi et al 1998). Since the Fe line must be associated with a reflection continuum, in all subsequent fits we always include a constant and neutral reflection model from Magdziarz & Zdziarski (1995) and a narrow Fe line. The reflection continuum normalization is chosen such that the Fe line equivalent width (with respect to such continuum only) is consistent with the *BeppoSAX* observation (EW$_{FeK}$ $\sim$700 eV) by Guainazzi et al (1998).

The strongest feature in the rms spectrum during the low flux observation (right panel of Fig. 2) is the drop of variability at $\sim$0.9 keV. In the pn spectrum of the low flux observation an emission–like feature with energy of 0.88 ± 0.02 keV and a flux of $(1.2 \pm 0.2) \times 10^{-4}$ ph s^{-1} cm^{-2} is present. This emission line is present also in previous *Chandra* low flux spectra as well (Collinge et al 2001; Uttley et al 2003). The energy of the feature in the pn spectrum is consistent with Ne IX (and possibly Fe emission plus O VIII recombination continuum, or RRC). A second feature is also detected around 0.5–0.6 keV, where emission from O VII and O VIII is expected. As already shown by Pounds et al (2004) the high–resolution RGS

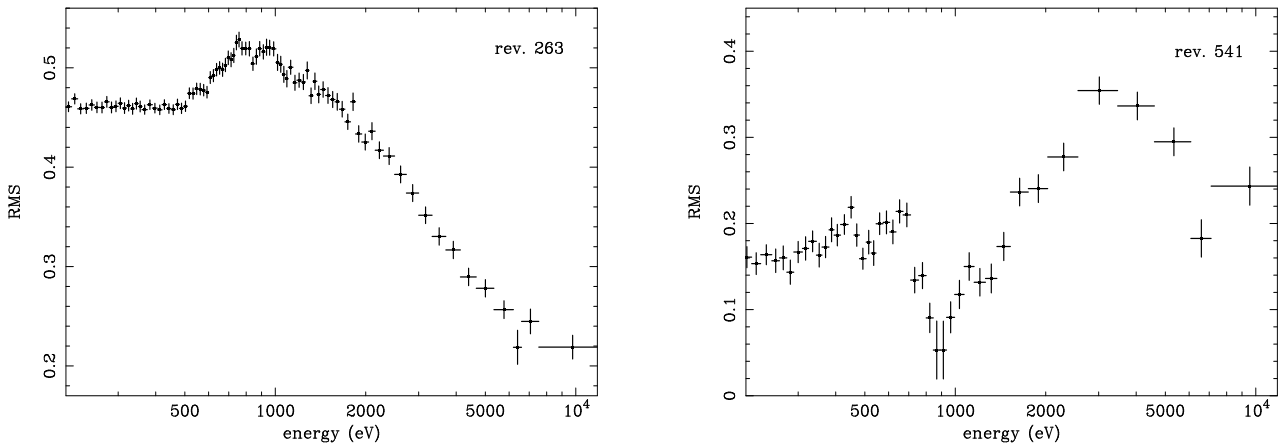

Figure 2. The RMS spectra of the rev. 263 (left panel) and rev. 541 (right panel). The RMS spectra are computed with time bins of 2 ks with a minimum of 300 counts per energy bin.

data during the same low flux *XMM–Newton* observation indeed show an emission line spectrum which is very similar to that of typical Seyfert 2 galaxies. The most prominent emission lines are due to the O VII triplet , the O VIII Kα line and the N VII Kα line. The Ne IX (forbidden) line is also clearly detected at 0.905 keV with a flux of $(3.5 \pm 1.0) \times 10^{-5}$ ph s^{-1} cm^{-2}. The intensity of this line is not enough to account for the pn feature around 0.9 keV. However, the Ne line sits on top of a broad feature most likely due to O VIII RRC and possibly unresolved Fe emission lines. When fitted with a crude Gaussian model in the RGS data, such a feature has an energy of 0.88 ± 0.01 keV and a flux of $(5.0 \pm 1.5) \times 10^{-5}$ ph s^{-1} cm^{-2}. By combining the Ne line with this broad feature ($\sigma \simeq 20$ eV) we obtain a flux of (0.7-1.1)$\times 10^{-4}$ ph s^{-1} cm^{-2} around 0.9 keV consistent with the pn lower limit. As mentioned in Pounds et al (2004) excess absorption might be present around 0.76 keV (possibly related to a M–shell unresolved transition array from Fe). If included in both CCD and RGS data, this has the effect of reducing the broad 0.9 keV feature intensity, making so more difficult to reproduce the variability drop in the RMS spectra.

3. TIME–RESOLVED SPECTRAL ANALYSIS

We then explore time–resolved spectroscopy on the shortest possible timescale (set by requiring good quality time–resolved individual spectra). In the following, we present results obtained by performing such an analysis on a 2 ks timescale (about four dynamical timescales at 10 r_g). The 2 ks slices that have been used in the analysis are shown in Fig. 1 and have been numbered for reference.

3.1. The 2–10 keV Γ–flux relationship

It is well known that the 2–10 keV spectral slope in NGC 4051 (and other sources) is correlated with the source flux. In Fig. 3, we show such a correlation when all the 2 ks spectra are fitted with a simple power–law model in the 2–10 keV band (including the constant reflection component from distant material discussed in Sec. 2). Data for the two observations are shown with different symbols.

The photon index increases with flux and seems to saturate at high flux around $\Gamma \simeq 2.2$ and at low fluxes to $\Gamma = 1.3$–1.4, with a $\Delta\Gamma \simeq 0.8$. Since the two asymptotes are not extremely well defined, such behaviour could still be consistent with spectral pivoting. On the other hand, the Γ–flux relationship can be explained if an additional and weakly variable component is present in the 2–10 keV band. If so, such a component dominates the low flux states and the hard photon index measured there is just a measure of its intrinsic spectral shape in the 2–10 keV band, while it is overwhelmed by the power law at high fluxes where $\Gamma \simeq 2.2$ is then the intrinsic power law photon index. In other words, as an alternative to spectral pivoting, the Γ–flux relationship can be explained by assuming the presence of i) a variable power law with constant or weakly variable slope $\Gamma \simeq 2.2$; ii) an additional less variable component with approximate spectral shape of $\Gamma = 1.3$–1.4 in the 2–10 keV band.

3.2. Broadband analysis I: the standard model

As a first step, we consider a simple continuum model comprising a power law plus black body (BB) emission to model the prominent soft excess. This is, in many respects, the "standard model" to fit AGN X–ray spectra and, though often crude and phenomenological, provides useful indications that can guide further analysis. The power law slope is free to vary to account for possible spectral pivoting. We add to the model neutral photoelec-

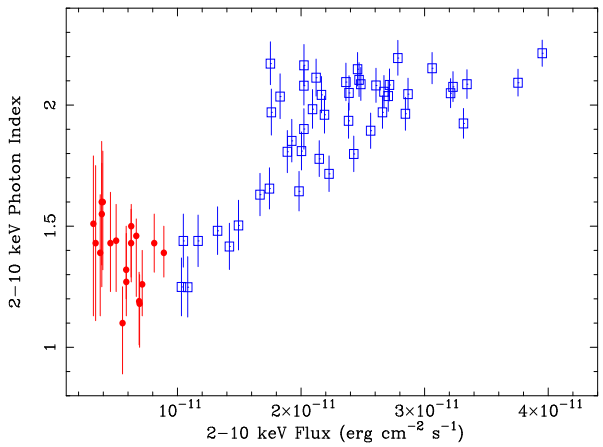

Figure 3. The best fit spectral index vs. flux in the 2–10 keV band. The contribution of the constant reflection (including a narrow Fe line) coming from distant material is considered in the model.

tric absorption with column density fixed to the Galactic value. To account for the presence of absorbing ionized gas in the line of sight we include two edges (O VII and O VIII). We searched for possible variations of their energies without finding any evidence, so we fixed the absorption energies to the rest–frame ones. This is clearly a crude approximation for the effects of the warm absorber in NGC 4051, but the quality of the individual 2 ks spectra is not such as to suggest the use of more sophisticated models. In addition, the constant components discussed above (reflection from distant matter and emission from photoionized gas) are also included in the spectral model. The overall model has six free parameters only. The resulting fits are very good with a reduced χ^2 ranging between 0.9 and 1.2 with a mean close to unity. Therefore, from a statistical point of view, a single model is able to describe the spectral variability of the source in a very satisfactory way.

In Fig. 4 (left panel) we show the relation between the measured BB temperature and its intensity, which is proportional to the luminosity (in the present case A_{BB}=10^{-4} correspond to L_{BB}=9.7×10^{40} ergs s^{-1}, assuming H_0=71 Mpc km^{-1} s^{-1}). The BB luminosity spans about one order of magnitude, while the BB temperature ranges from about 90 eV to 140 eV with an average of 110–120 eV. Such a temperature is somewhat high, but can still be consistent with that expected from a black hole with mass $\simeq 5 \times 10^5\ M_\odot$ (Shemmer et al 2003; M$^{\rm c}$Hardy et al 2004) accreting at high rate. If the soft excess in NGC 4051 is really due to BB emission from a constant area, we should be able to detect the BB law ($L_{BB} \propto T^4$) in data spanning one order of magnitude in BB luminosity. However, such a relation is ruled out ($\chi^2 = 1552$ for 67 degrees of freedom). The relation appears to be much steeper (with an index of 6.3–6.4 rather than 4), but even so, a power law fit is unacceptable. Moreover the measured temperature appears to be much more constant (the fit with a constant gives a $\chi^2 = 75$ for 67 degrees of freedom) than predicted by standard disc models.

The properties of the soft excess in NGC 4051 are remarkably similar to those of 26 bright radio–quiet quasars studied e.g. by Gierlinski & Done (2004). The quasar sample spans a wide range of black hole masses and luminosities and should therefore exhibit a wide range of disc temperatures. However, the measured temperature of the soft excess is remarkably constant throughout the sample with a mean of 120 eV (and very small variance). It is a rather surprising coincidence that this is exactly the average temperature we measure for the soft excess in NGC 4051, considering that the black hole mass in NGC 4051 is about 3 orders of magnitude smaller than the typical black hole mass in the quasar sample.

The "standard model" of the source emission seems to be inadequate to describe the corona parameters as well. In the right panel of Fig. 4 we show the power law slope as a function of the 0.5–10 keV flux. In the normal/high flux observation the photon index steepens with flux, as already pointed out in the 2–10 keV analysis. This behaviour is consistent with spectral pivoting, even if the lowest Γ require a too hard spectral shape to be accounted for by standard Comptonization models. The main problems arise at very low fluxes, where the Γ–flux relation is inverted in a manner that is not consistent with simple spectral pivoting. Such behaviour could indicate the presence of an additional soft (steep) component which becomes prominent at low fluxes and is not properly accounted for by the black body component. In fact, the power law is trying to fit the soft data by steepening the index at low fluxes and leaves significant residuals in the hard band where a slope of about 1.3–1.4 would be more appropriate even at very low fluxes (see Fig. 3).

Such discrepancies naturally raises questions on the real nature of the X–ray soft excess and of the soft steep component observed at low fluxes. As pointed out by Gierlinski & Done (2004), the remarkable constancy of the "soft excess temperature" might indicate an origin in atomic rather than thermal physical conditions. Possible candidates seems to be absorption and/or ionized reflection. We investigate here the two–component model in which the soft excess and the soft steep component observed at low fluxes are due to a ionized reflection component.

3.3. Broadband analysis II: the two–component model

In the two–component model the variability is dominated by a power law component (PLC) which changes in flux but not in spectral shape ($\Gamma = 2.2$). The PLC illuminates the accretion disc giving rise to a reflection–dominated component (RDC, from Ross & Fabian 2005) which is affected by the relativistic effects arising in the inner disc. We take into consideration these effects convolving the ionized reflection spectrum with a LACR kernel with fixed inner and outer disc radius (to $1.24\ r_g$ and $100\ r_g$ respectively), and fixed disc inclination (30°). The inner disc

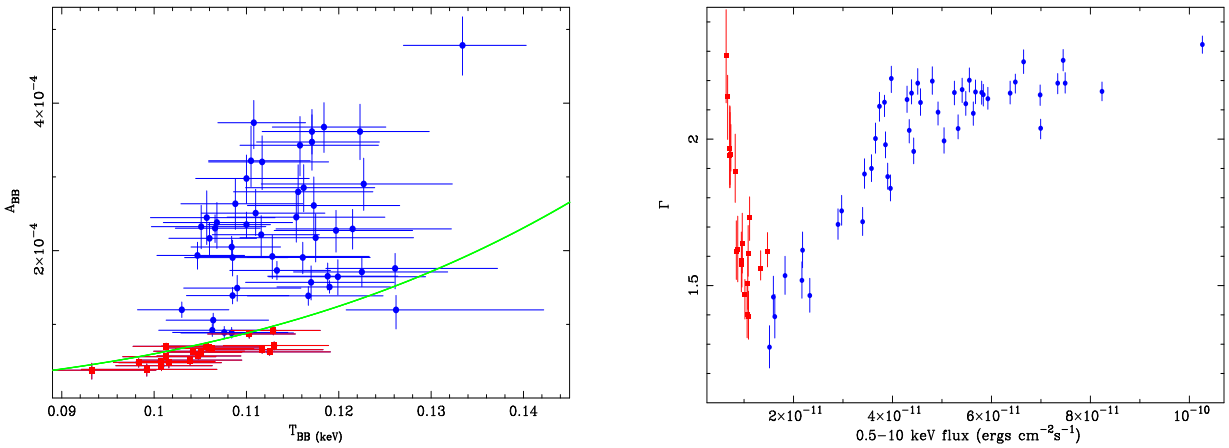

Figure 4. In the left panel we show the blackbody intensity as a function of its observed temperature. The line shows the best fit relation between the $A_{BB} \propto T_{BB}^4$. In the right panel, we show the broadband Γ–flux relationship as obtained from the standard model fits (see text for details).

radius corresponds to the innermost stable circular orbit around a Kerr black hole. The only free parameters of the relativistic kernel is then the index q of the disc emissivity profile ($\epsilon = r^{-q}$). The ionized reflection model is appropriate for solar abundances and has ionization parameter and normalization as free parameters, while the photon index of the illuminating power law in the RDC model is tied to that of the PLC and therefore fixed to $\Gamma = 2.2$. As for the "standard model" discussed in the previous Section, the overall spectral model also includes Galactic absorption, constant emission from photoionized gas and from a distant reflector and the O VII and O VIII edges with fixed energies. The number of free parameters in the model is just the same as in the "standard model" case (6 free parameters).

The model reproduces very well the data at all flux levels with a reduced χ^2 between 0.8 and 1.2. The two–component model is statistically indistinguishable from the standard one and has to be considered as a possible alternative to be accepted or rejected on a physical rather than statistical basis. We would like to stress again that with this interpretation the soft excess is not due to a thermal component anymore. It is the ionized reflection from the disc that naturally produces a soft excess. The reflection can then naturally solve the "constant temperature" problem because of the very non–thermal nature of that component. Moreover, no changes in the PLC slope are required to fit the data and to reproduce the Γ–flux relation. We tested, in fact, a variable Γ fit to the data and found that all the 68 spectra are consistent with Γ=2.2 with only three exceptions (with $\Delta\Gamma$ <0.1). Thus, the Γ–flux relation is simply due to the relative contribution of the two components, with the steep and variable PLC dominating the medium and high flux states and with a stronger contribution of the flatter RDC during the low flux ones.

As for the variability of the two components, the RDC is expected to respond to the PLC variations and to be well correlated with it. Fig. 5 shows the 0.5–10 keV flux of the RDC versus the PLC flux in the same band. The RDC is well correlated with the PLC at low flux levels (the solid line represent perfect correlation between the two components). However, as the PLC flux increases, the correlation clearly breaks down and the RDC is much less variable (about a factor 2.5) than the PLC (about a factor 7). A similar behaviour has been observed also in MCG-6-30-15 (Vaughan & Fabian 2004) and has been interpreted in terms of a strong gravitational light bending by Miniutti et al (2003) and Miniutti & Fabian (2004), which predicts an almost stable RDC during normal/high flux periods and a correlation at low flux levels only. The observed variability is therefore in good agreement with the light bending model prediction. The other free parameters of the RDC in our fit are the disc reflection emissivity index of the relativistic blurring model (q) and the ionization parameter of the reflection spectrum (ξ). The former shows some trend with flux, with low flux states generally corresponding to steeper emissivity profiles than high flux ones (Ponti et al. in prep.). This result is also in line with the predictions of the light bending model (Miniutti & Fabian 2004). The latter, instead, is not very well constrained by the data and most spectra are consistent with ξ between 50 and 300 erg cm s^{-1} with only few exceptions below and above (and no clear trend with flux). We finally remark that, if the light bending interpretation is correct, the RDC versus PLC behaviour requires the primary source of PLC to be centrally concentrated above the accretion disc within 15 gravitational radii at most from the central black hole (see Miniutti & Fabian 2004). In particular, the correlation between the two component is predicted to occur only if the primary source of the PLC is within $\sim$ 5 gravitational radii from the hole. Therefore, one consequence of this interpretation is that low flux states are characterised by an extremely compact region of primary emission, well inside the relativistic region around the black hole.

As a final comment, the mean optical depth of the ionized absorber, here modelled crudely by the O VII and O VIII edges, is of the order of 0.1–0.2. These values are

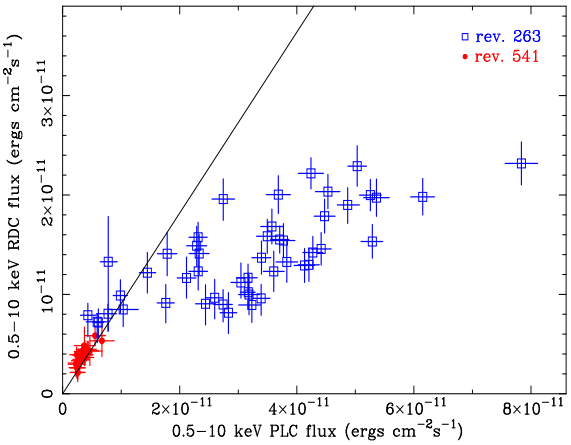

Figure 5. RDC vs. PLC 0.5–10 keV fluxes. The data clearly rule out a perfect correlation between the two components (solid line). The RDC is well correlated with the PLC at low fluxes only and varies with smaller amplitude in normal/high flux states.

left free to vary and they seem to suggest some variations during the two observations (in agreement with the evidences presented by Elvis et al. during this conference). Nevertheless, the uncertainties associated with our measurements are so large that a fit to the optical depth with a constant during the first observation results in a χ^2 of 26 (O VII) and 47 (O VIII) for 47 degrees of freedom, while during the second low flux observation the χ^2 are 29 and 7 for 19 degrees of freedom, preventing us from claiming the variation.

4. CONCLUSIONS

We investigated the X–ray spectral variability of the Narrow Line Seyfert 1 galaxy NGC 4051 with model independent techniques (RMS spectra and Flux–Flux plots) and with time resolved spectral variability. NGC 4051 show evidence for a distant neutral and constant reflection component contributing by about 10 per cent in the 4–10 keV band at mean fluxes and constant emission from photoionized gas.

The nuclear emission has been interpreted both in a "standard scenario" (consisting of BB plus power law emission) and by a two–component (PLC plus ionized RDC from the disc). Both models reproduce the RMS spectra, and describe the time–resolved spectra in a comparable way from a statistical point of view, thus the dinstinction has to be made on a physical basis. In the framework of the two–component model the soft excess is interpreted as the soft part of ionized reflection from the accretion disc. The constant temperature problem is then solved in terms of atomic rather than truly thermal processes. Moreover, the RDC explains the Γ–flux relationship at all flux levels in terms of the relative contribution of a PLC with constant slope $\Gamma = 2.2$ and the RDC.

REFERENCES

Collinge M.J. et al, 2001, ApJ, 557, 2

Edelson et al, 2002, ApJ, 568, 610

Gierliński, M., & Done, C., 2004, MNRAS, 349, L7

Guainazzi M. et al, 1998, MNRAS, 301, L1

Haardt, F., & Maraschi, L., 1991, ApJL, 380, L51

Haardt, F., & Maraschi, L., 1993, ApJ, 413, 507

Haardt, F., Maraschi, L., & Ghisellini, G., 1997, ApJ, 476, 620

Lamer G. et al., 2003, MNRAS, 338, 323

M^{c}Hardy I.M. et al., 2004, MNRAS, 348, 783

Magdziarz P., Zdziarski A.A., 1995, MNRAS, 273, 837

Markowitz A., Edelson R., Vaughan S., 2003, ApJ, 598, 935

Miniutti, G., Fabian, A. C., Goyder, R., & Lasenby, A. N. 2003, MNRAS, 344, L22

Miniutti, G., & Fabian, A. C., 2004, MNRAS, 349, 1435

Ponti, G., Cappi, M., Dadina, M., & Malaguti, G., 2004, A&A, 417, 451

Ponti, G., et al, 2005, Proceedings of the 6th Italian Conference on Active Galactic Nuclei, http://www.arcetri.astro.it/ agn6/

Pounds K.A., Reeves J.N., King A.R., Page K.L., 2004, MNRAS, 350, 10

Poutanen, J., & Fabian, A. C. 1999, MNRAS, 306, L31

Ross, R. R., & Fabian, A. C., 2005, MNRAS, 358, 211

Shemmer O., Uttley P., Netzer H., M^{c}Hardy I.M, 2003, MNRAS, 343, 1341

Shih, D. C., Iwasawa, K., & Fabian, A. C., 2002, MNRAS, 333, 687

Uttley P., Fruscione A., M^{c}Hardy I.M., Lamer G., 2003, ApJ, 595, 656

Uttley P., et al, 2004, MNRAS, 347, 1345

Vaughan, S., Edelson, R., Warwick, R. S., & Uttley, P., 2003, MNRAS, 345, 1271

Vaughan, S., & Fabian, A. C., 2004, MNRAS, 348, 1415